Available online at www.sciencedirect.com
ScienceDirect
Journal of Organometallic Chemistry 692 (2007) 5717–5726
Journal of Organometallic Chemistry
www.elsevier.com/locate/jorganchem

Carbonyl complexes of manganese, rhenium and molybdenum with 2-pyridylimino acid ligands

Celedonio M. Alvarez, Raúl García-Rodríguez, Daniel Miguel *

IU CINQUIMA/Química Inorgánica, Facultad de Ciencias, Universidad de Valladolid, E-47005 Valladolid, Spain

Received 3 August 2007; received in revised form 25 September 2007; accepted 25 September 2007
Available online 1 October 2007

Abstract

[$MBr(CO)_3\{\kappa^2(N,O)$-pyca}] [M = Mn(**1a**), Re(**1b**), pyca = pyridine-2-carboxaldehyde] and [$MoCl(\eta^3$-C_3H_4Me-2)$(CO)_2\{\kappa^2(N,O)$-pyca}] (**1c**) react with aminoacid β-alanine to give the corresponding iminopyridine complexes **2a**–**2c**. The same method affords the iminopyridine derivatives from γ-aminobutyric acid (GABA) (**3a**–**3c**) and 3-aminobenzoic acid (**4a**–**4c**). For complexes **2a**–**2c**, **3a**, **3c** and **4a**, the solid state structures have been determined by X-ray crystallography, revealing interesting differences in their hydrogen-bonding patterns in solid state.

Keywords: Pyridylimino acid ligands; Carbonyl complexes; Schiff bases

1. Introduction

Bioorganometallic chemistry is currently attracting a great deal of attention particularly in the field of labeling of biomolecules [1] since organometallic bioconjugates can be detected by a variety of methods including infrared and optical spectroscopy [2], immunoassays [3], electrochemistry [4], radioimaging [5], or luminescence [6].

We have published recently the preparation of a family of Mo(0) complexes where the introduction of α-amino acids in the formation of iminopyridines led, as a side reaction, to the loss of the acid group *via* decarboxylation upon coordination to the metal atom [7]. The introduction of a phenyl group or an additional carbon atom adjacent to the α-carbon of the amino acid, led to complexes which turned to be stable towards decarboxylation. We thought it to be of interest to extend the method to build complexes with other metal–ligand fragments containing a stable carboxylic acid function that could be used to bind biomolecules (peptides, proteins, etc.) [8]. This would open the way for their use as probes in which the metal and the surrounding ligands provide the spectroscopic properties suitable for their observation [9]. Most promising in this field are UV–Vis spectroscopy and, particularly, IR spectroscopy since the carbonyl ligands attached to the metal produce strong and very sensitive stretching bands. Additionally, such complexes may help to study the hydrogen bond interactions [10] responsible for the structure of proteins and other supramolecular systems [11]. In this respect, considerable attention has been paid to the H-bonding arrangement of simple organic carboxylic acids and amides attempting to establish patterns for crystal engineering [12]. The studies have been extended to metal complexes containing these functionalities [13], and a study of hydroxyl containing iminopyridine ligand has also been reported [14].

Following pioneering studies from Alberto et al. [15], we have recently developed a new methodology for the synthesis of pyridylimino complexes using the carbonyl compounds [$MBr(CO)_3\{\kappa^2(N,O)$-pyca}] [M = Mn(**1a**), Re(**1b**), pyca = pyridine-2-carboxaldehyde] and [$MoCl(\eta^3$-C_3H_4Me-2)$(CO)_2\{\kappa^2(N,O)$-pyca}] (**1c**) as starting complexes [16]. This methodology permits a wide range of

* Corresponding author. Tel.: +34 983 184096; fax: +34 983 423013.
E-mail address: dmsj@qi.uva.es (D. Miguel).

0022-328X/$ - see front matter © 2007 Elsevier B.V. All rights reserved.
doi:10.1016/j.jorganchem.2007.09.025

functionalization of the pyridylimino ligand due to the use, if necessary, of very mild reaction conditions and a broad range of solvents.

We present here the use of complexes **1a**–**1c** for the preparation and characterization of new complexes of manganese, rhenium and molybdenum with iminopyridine ligands derived from the amino acids β-alanine, γ-aminobutyric acid (GABA) and 3-aminobenzoic acid. GABA is an important inhibitor which acts in a wide variety of biological processes, whereas β-alanine, the simplest β-amino acid (and the only one occurring naturally) is believed to be involved in the visual system [17] and, together with GABA, to act as a neurotransmitter in the central nervous system [18]. A series of complexes of the $W(CO)_4$ fragment containing iminopyridines derived from 3-aminobenzoic acid [19] and a series of amino acids and dipeptides [20] have been recently reported, as well as the bromo tricarbonyl rhenium iminopyridine derivative of ω-amino undecanoic acid [21].

2. Results and discussion

2.1. Preparation and characterization of complexes

Complexes **1a**–**1c**, containing pyridine-2-carboxaldehyde acting as κ^2(N,O) bidentate chelate, react with the appropriate amino acids to afford iminopyridine complexes **2a**–**2c** (derived from β-alanine), **3a**–**3c** (derived from GABA) or **4a**–**4c** (derived from 3-aminobenzoic acid) as shown in Scheme 1.

For Mn and Re complexes **2a** and **2b**, **3a** and **3b** and **4a**–**4b**, the reactions were carried out in refluxing ethanol for 1 h. In the case of Mo complexes **4a**–**4c** the reactions could be done in THF/methanol mixture due to their better solubility. All these reactions can be carried out at room temperature but the increase of the temperature speeds up the reactions because of the increment of the amino acids solubility.

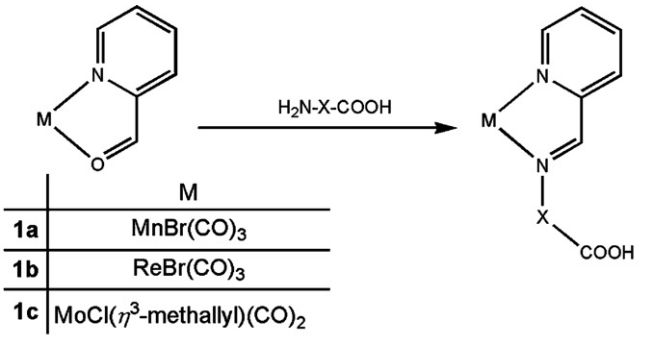

	M
1a	$MnBr(CO)_3$
1b	$ReBr(CO)_3$
1c	$MoCl(\eta^3\text{-methallyl})(CO)_2$

X \ M	$MnBr(CO)_3$	$ReBr(CO)_3$	$MoCl(\eta^3\text{-methallyl})(CO)_2$
$-(CH_2)_2-$	**2a**	**2b**	**2c**
$-(CH_2)_3-$	**3a**	**3b**	**3c**
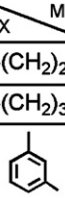	**4a**	**4b**	**4c**

Scheme 1.

All complexes have been characterized by analytical and spectroscopic methods. IR spectra in solution show the expected patterns of ν(CO) stretching bands for the carbonyl ligands and the carboxylic acid function (see Section 3). For complexes **2a**–**2c**, **3a**, **3c** and **4a**, the solid state structures have been determined by X-ray crystallography.

The results are displayed in Figs. 1–5 and the crystal and refinement data are collected in Table 1. A comparison of the most relevant distances is given in Table 2. In all the structures, the coordination around the metal is reminiscent of that found in other iminopyridine complexes bearing side chains with different functionalities such as ester [15,16,22], carboxylate [7], hydroxyphenyl [23], or ethynylphenyl [23]. However, the most interesting features of the structures concern to the hydrogen-bonding arrangement of the acids in solid state, as discussed in Section 2.2 below. Analysis of ^{1}H NMR spectra together with structural data and some additional experiments helped to assign the structures of the remaining complexes **3b** and **4b** and **4c** (see Section 2.3 below).

2.2. Hydrogen-bonding arrangement in solid state

Mn and Re complexes show the same behaviour, adopting the well-known centrosymmetric-dimer arrangement through H-bonding involving both the =O and –OH groups of the carboxylate unit in a complementary manner, as seen in Fig. 1 (compounds **2a** and **2b**), Fig. 3 (compound **3a**) and Fig. 5 (compound **4a**). The C=O···O distances range from 2.569 to 2.687 Å.

In all these Mn and Re complexes, the chain bearing the carboxylic acid functions is placed nearly antiparallel to the M–Br axis. In contrast, the structures of molybdenum complexes **2c** and **3c** display a different disposition, with the carboxylic acid arms nearly coplanar to the iminopyridine system.

The H-bonding arrangement for the molybdenum complexes is remarkably different from that found for Mn and Re complexes described above. In the solid state structure of **2c** (Fig. 2) there is a centrosymmetric dimeric arrangement of two molecules of the complex together with two molecules of methanol in which the hydroxyl groups of methanol serve as bridges (carboxylic)O–H···O(methanol)-H···Cl, between the hydroxyl groups of the carboxylic acid and the chlorine atom of the adjacent molecule, in a complementary manner (see Fig. 2, bottom). Complex **2c** shows a strong tendency to incorporate polar solvents. Despite repeated attempts, it was not possible to grow crystals without solvent molecules. In one occasion, after several weeks in the refrigerator, crystals of **2c** were obtained which contained a water molecule (from adventitious humidity). The structure of this hydrate was measured and solved, to show an arrangement similar to that described for the methanol solvate [24].

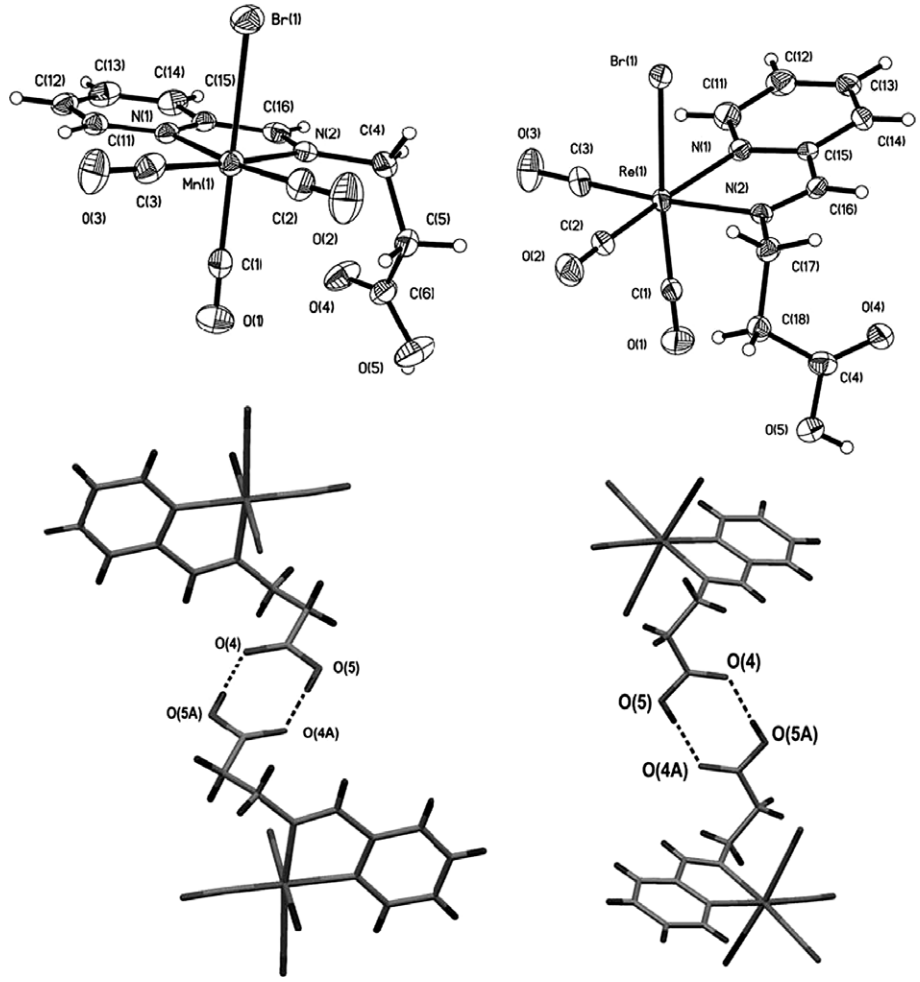

Fig. 1. (Above) ORTEP plots (30% ellipsoid probability) for compounds **2a** (left) and **2b** (right). (Below) Mercury drawings showing the H-bonding arrangement for **2a** (left) and **2b** (right). Selected distances (Å) and angles (°): Compound **2a**: Mn(1)–Br(1) 2.5271(11), C(6)–O(4) 1.203(6), Mn(1)–N(1) 2.041(4), C(6)–O(5) 1.287(6), Mn(1)–N(2) 2.047(4), C(1)–Mn(1)–Br(1) 179.23(15), Mn(1)–C(1) 1.829(6), C(2)–Mn(1)–N(1) 174.12(19), Mn(1)–C(2) 1.816(6), C(3)–Mn(1)–N(2) 173.30(18), Mn(1)–C(3) 1.803(6), N(1)–Mn(1)–N(2) 78.49(15). Hydrogen bonds: H(5)···O(4A) 1.79(6), O(5)···O(4A) 2.687(6), O(5)–H(5)···O(4A) 157.7. Compound **2b**: Re(1)–Br(1) 2.621(2), C(4)–O(4) 1.206(10), Re(1)–N(1) 2.169(6), C(4)–O(5) 1.320(10), Re(1)–N(2) 2.157(6), C(1)–Re(1)–Br(1) 175.0(2), Re(1)–C(1) 1.919(9), C(2)–Re(1)–N(1) 171.3(3), Re(1)–C(2) 1.923(9), C(3)–Re(1)–N(2) 173.6(3), Re(1)–C(3) 1.894(9), N(1)–Re(1)–N(2) 75.0(2). Hydrogen bonds: H(5)···O(4A) 1.74(6), O(5)···O(4A) 2.674(10), O(5)–H(5)···O(4A) 178.5(5).

Complex **3c** displays an arrangement which is very different both from the "normal" dimers found for the Mn and Re complexes, or the methanol bridged dimers found for **2c.** It consists of infinite helicoidal chains in which the molecules are linked through H-bonding involving the terminal carboxylic hydroxyl O(5)–H(5) to the chlorine atom Cl(1A) of the adjacent molecule related to the former by a twofold screw axis. The arrangement propagates along the 2_1 axis, thus completing a turn of the helix every two molecules (see Fig. 4). This very unusual feature could be due to the higher electronegativity of chlorine atom compared to bromine.

2.3. NMR Spectroscopy structural determination

^{1}H NMR spectra for compounds **2a**–**2c**, **3a**, **3c** and **4a** are consistent with the structures obtained using X-ray diffraction, pointing out that their structures are maintained in solution. The pattern and the frequencies showed by all the ^{1}H NMR spectra are those expected for the ligands coordinated to the metal centers. The pyridylimino moiety shows 5 characteristic signals between 10 and 6 ppm. Chemical shifts (δ) are recorded in Table 3 and the labeling used can be found in Fig. 6.

The structure of the compounds **3b**, **4b** and **4c** could be inferred from NMR experiments. ^{1}H NMR spectrum of complex **3b** in acetone-d_6 displays, in addition of the pyridylimino signals, three multiplets due to the aliphatic CH_2 protons at 4.26, 2.50 and 2.33 ppm. A ^{1}H-^{1}H COSY NMR experiment was carried out on complex **3b** to help in the assignment of the proton chemical shifts (Fig. 7). In this experiment, besides the set of cross peaks observed for the pyridyl and the aliphatic groups, one cross peak between the imino proton (H_1) and the CH_2 protons bonded to the N atom can be observed.

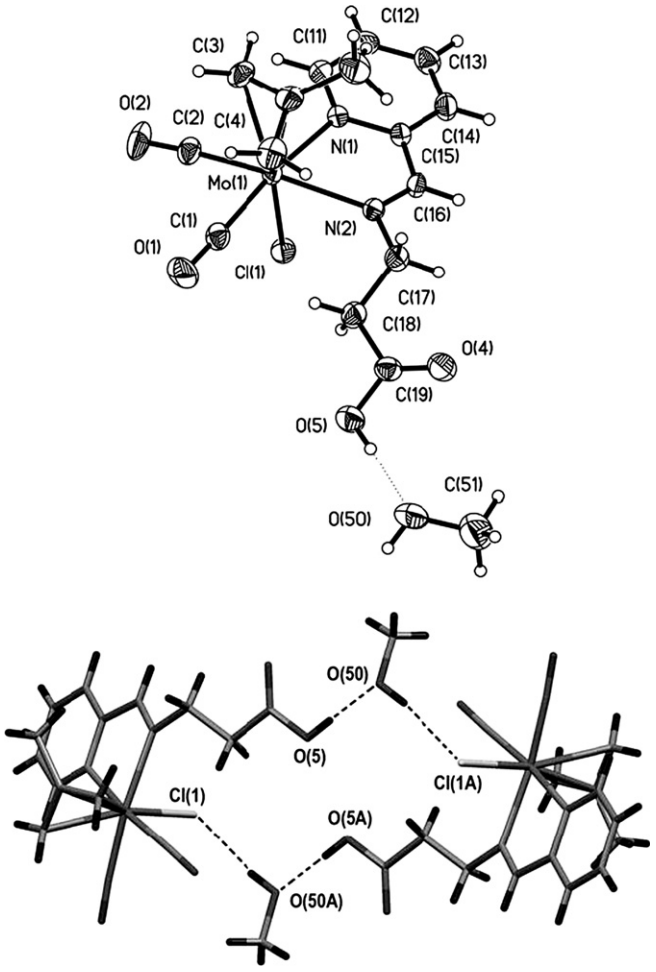

Fig. 2. (Above) ORTEP plot (30% ellipsoid probability) for compound **2c**. (Below) Mercury drawing showing the H-bonding arrangement for **2c**. Selected distances (Å) and angles (°): Mo(1)–Cl(1) 2.5028(9), O(4)–C(19) 1.183(4), Mo(1)–N(1) 2.237(2), O(5)–C(19) 1.314(4), Mo(1)–N(2) 2.256(2), C(1)–Mo(1)–N(1) 168.62(12), Mo(1)–C(1) 1.946(4), C(2)–Mo(1)–N(2) 166.04(11), Mo(1)–C(2) 1.955(4), C(4)–Mo(1)–Cl(1) 164.75(10), Mo(1)–C(4) 2.241(3), N(1)–Mo(1)–N(2) 73.56(9). Hydrogen bonds: H(50)···Cl(1A) 2.181(6), O(50)···Cl(1A) 3.111(3), O(50)–H(50)···Cl(1A) 171.1(2), H(5)···O(50) 1.26(9), O(5)···O(50) 2.663(5), O(5)–H(5)···O(50) 176.6(2).

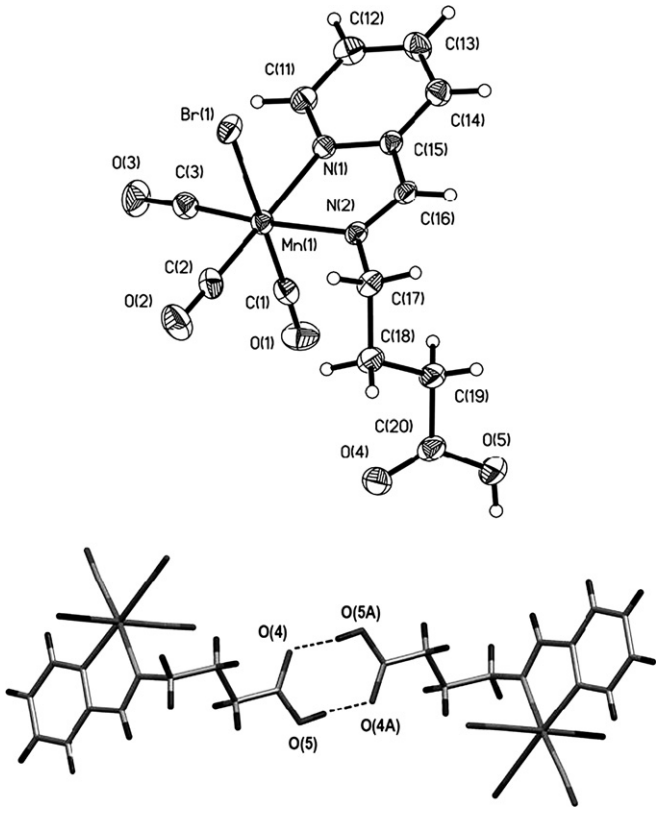

Fig. 3. (Above) ORTEP plot (30% ellipsoid probability) for compound **3a**. (Below) Mercury drawing showing the H-bonding arrangement for **3a**. Selected distances (Å) and angles (°): Mn(1)–Br(1) 2.5352(11), C(20)–O(4) 1.221(8), Mn(1)–N(1) 2.048(5), C(20)–O(5) 1.293(7), Mn(1)–N(2) 2.041(4), C(1)–Mn(1)–Br(1) 177.7(2), Mn(1)–C(1) 1.791(7), C(2)–Mn(1)–N(1) 172.7(2), Mn(1)–C(2) 1.803(7), C(3)–Mn(1)–N(2) 173.8(2), Mn(1)–C(3) 1.791(7), N(2)–Mn(1)–N(1) 78.35(18). Hydrogen bonds: H(5)···O(4A) 1.718(9), O(5)···O(4A) 2.636(7), O(5)–H(5)···O(4A) 165.2(4).

Complexes **4b** and **4c** present more crowded aromatic regions. Additionally, in the case of compound **4c**, five signals due to the methallyl protons are observed. The signal at 1.42 ppm was assigned to the methyl group showing two more shielded signals (1.27 and 1.04 ppm) due the *anti* protons and two less shielded signals (2.90 and 2.22 ppm) due the *syn* protons. Analysis of the ^1H–^1H COSY NMR cross peaks indicate the presence of the two aromatic rings and permitted the assignment of the signals of their protons. The same experiment on compound **4b** displays two *anti*/*syn* sets of protons bonded to the same carbon atom. The acidic proton signals appear in the range from 12 to 10 ppm as expected (Table 3).

The broad shape of the signals reveals the occurrence of some dynamic process. Usually, the process involving these acidic protons is the exchange with H_2O protons. To prove this assumption, a ^1H–^1H EXSY NMR experiment (mixing time of 200 ms) on the compound **3b** has been carried out showing a cross peak between the acidic proton and the residual H_2O signals (Fig. 8).

2.4. Conclusion

Complexes containing pyridine-2-carboxaldehyde as chelate κ^2(N,O) ligand can be used as convenient starting materials for the preparation of iminopyridine complexes containing a carboxylic acid pendant arm by high-yield reactions with the amino acids β-alanine, γ-aminobutyric acid (GABA) and 3-aminobenzoic acid, in a facile, high-yield synthetic method in mild conditions. The structure determinations reveal that the H-bonding patterns in solid state are strongly dependent on the nature of the metal. Thus for the bromotricarbonyl complexes of Mn(I) and Re(I) is found the well-known centrosymmentric dimeric arrangement. In contrast, complexes containing the (methallyl)chlorodicarbonylmolybdenum(II) fragment, display unusual arrangements of infinite chains involving chlorine atoms, or macrocycles involving both chlorine atoms and polar solvents such as methanol or water.

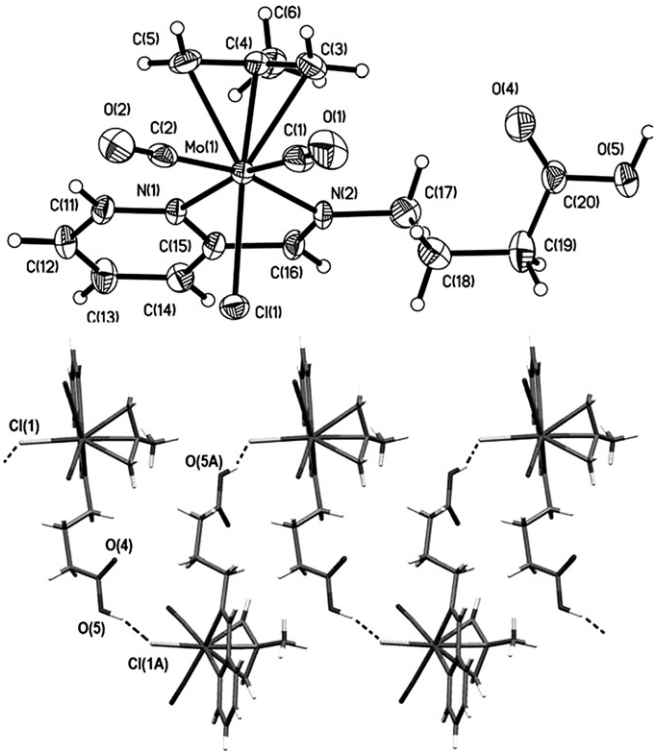

Fig. 4. (Above) ORTEP plot (30% ellipsoid probability) for compound **3c**. (Below) Mercury drawing showing the H-bonding arrangement for **3c**. Selected distances (Å) and angles (°): Mo(1)–Cl(1) 2.5027(17), O(4)–C(20) 1.195(7), Mo(1)–N(1) 2.237(4), O(5)–C(20) 1.304(7), Mo(1)–N(2) 2.260(4), C(1)–Mo(1)–N(1) 168.2(2), Mo(1)–C(1) 1.957(7), C(2)–Mo(1)–N(2) 167.7(2), Mo(1)–C(2) 1.946(7), C(4)–Mo(1)–Cl(1) 165.02(16), Mo(1)–C(4) 2.235(6), N(1)–Mo(1)–N(2) 72.96(15). Hydrogen bonds: H(5)···Cl(1A) 2.252(6), O(5)···Cl(1A) 3.141(4), O(5)–H(5)···Cl(1A) 158.1(3).

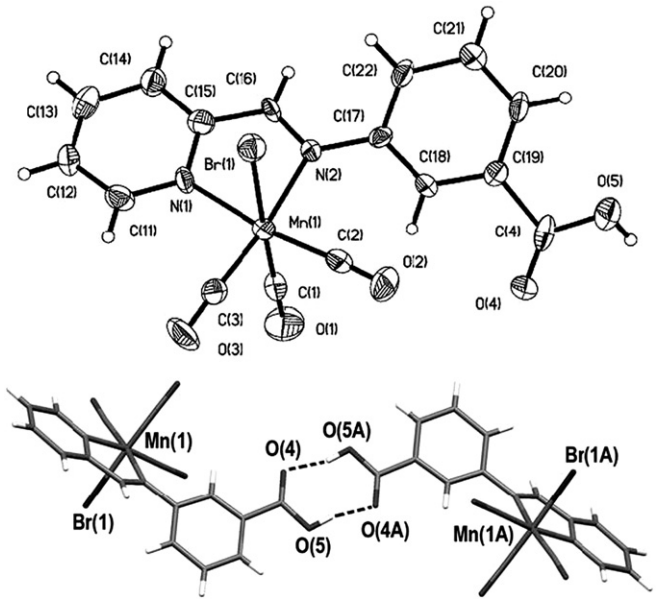

Fig. 5. (Above) ORTEP plot (30% ellipsoid probability) for compound **4a**. (Below) Mercury drawing showing the H-bonding arrangement for **4a**. Selected distances (Å) and angles (°): Mn(1)–Br(1) 2.524(3), C(4)–O(4) 1.17(2), Mn(1)–N(1) 2.053(11), C(4)–O(5) 1.32(2), Mn(1)–N(2) 2.056(12), C(1)–Mn(1)–Br(1) 178.3(5), Mn(1)–C(1) 1.80(2), C(2)–Mn(1)–N(1) 172.3(6), Mn(1)–C(2) 1.815(18), C(3)–Mn(1)–N(2) 173.0(6), Mn(1)–C(3) 1.83(2), N(1)–Mn(1)–N(2) 77.5(5). Hydrogen bonds: H(5)···O(4A) 1.73(1), O(5)···O(4A) 2.57(7), O(5)–H(5)···O(4A) 147.4(9).

3. Experimental

3.1. Materials and general methods

All operations were performed under an atmosphere of dry nitrogen using Schlenk and vacuum techniques. Details of the instrumentation and experimental procedures have been given elsewhere [25]. Literature procedures for the preparation of starting materials are quoted in each case. Ligands and other reagents were obtained from commercial sources and used without further purification unless otherwise stated.

3.2. Synthesis of *[MnBr(CO)$_3${py-2-CH=N–(CH$_2$)$_2$–COOH}] (**2a**)*

Compound **1a** [16] (0.120 g, 0.370 mmol) and β-alanine (0.033 g, 0.370 mmol) were refluxed in EtOH (25 ml) for 1 h. The solvent was evaporated *in vacuo*, and the resulting solid residue was dissolved in THF and filtered through kieselguhr. Addition of hexane and slow evaporation at reduced pressure gave compound **2a** as orange microcrystals. Yield: 0.109 g, 74%. Anal. Calc. for $C_{12}H_{10}BrMnN_2O_5$: C, 36.30; H, 2.54; N, 7.06. Found: C, 36.38; H, 2.44; N, 7.49%. IR (THF), *ν*(CO): 2024 (vs), 1938 (s), 1917 (s), 1734 (m) (acid) cm^{-1}. ^{1}H NMR (acetone-d_6): *δ* 10.65 (br, 1H, COO*H*), 9.25 [d(3), 1H, *H*^{6} py], 8.90 (br, 1H, –C*H*=N–), 8.21(br, 2H, *H*^{3,4} py), 7.76 (br, 1H, *H*^{5} py), 4.49 (br, 2H, *H*^{2} NCH_2), 3.58 (br, 2H, CH_2COOH).

3.3. Synthesis of *[ReBr(CO)$_3${py-2-CH=N–(CH$_2$)$_2$–COOH}] (**2b**)*

Compound **1b** [16] (0.120 g, 0.262 mmol) and β-alanine (0.024 g, 0.262 mmol) were refluxed in EtOH (25 ml) for 1 h. The solution turned deep red. The solvent was evaporated *in vacuo*, and the resulting solid residue was dissolved in THF and filtered through kieselguhr. Addition of hexane and slow evaporation at reduced pressure gave compound **2b** as orange microcrystals Yield: 0.118 g, 85%. Anal. Calc. for $C_{12}H_{10}BrN_2O_5Re$: C, 27.28; H, 1.91; N, 5.30. Found: C, 27.40; H, 2.18; N, 5.64%. IR (THF), *ν*(CO): 2022 (vs), 1923 (s), 1899 (s), 1734 (m) (acid) cm^{-1}. ^{1}H NMR (acetone-d_6): *δ* 10.70 (br, 1H, COO*H*), 9.25 (s, 1H, –C*H*=N–), 9.11 [d(5), 1H, *H*^{6} py], 8.32 (m, 2H, *H*^{3,4} py), 7.82 (m, 1H, *H*^{5} py), 4.42 [t(6), 2H, *H*^{2} NCH_2], 3.16 [q(7), 2H, CH_2COOH].

3.4. Synthesis of *[MoCl(η^3-C$_3$H$_4$Me-2)(CO)$_2${py-2-CH=N–(CH$_2$)$_2$–COOH}] (**2c**)*

Compound **1c** [16] (0.120 g, 0.343 mmol) and β-alanine (0.031 g, 0.343 mmol) were refluxed in THF (25 ml) and

Table 1a
Crystal data and refinement details for **2a**, **2b**, and **2c**

	2a	**2b**	**2c**
Empirical formula	$C_{12}H_{10}BrMnN_2O_5$	$C_{12}H_{10}BrN_2O_5Re$	$C_{16}H_{21}ClMoN_2O_5$
Formula weight	397.07	528.33	452.74
Crystal system	monoclinic	triclinic	monoclinic
Space group	$P2(1)/c$	$P\bar{1}$	$P2(1)/c$
a (Å)	15.165(6)	8.101(6)	7.4403(15)
b (Å)	7.960(3)	9.623(7)	24.897(5)
c (Å)	12.344(5)	10.758(8)	10.652(2)
α (°)	90	109.253(12)	90
β (°)	73.35(1)	90.944(14)	101.712(4)
γ (°)	90	105.381(15)	90
V (Å^3)	104.808(8)	758.4(10)	1932.1(6)
Z	4	2	4
T (K)	296(2)	296(2)	293(2)
D_{calc} (g cm^{-3})	1.831	2.314	1.556
$F(000)$	784	492	920
λ (Mo Kα) (Å)	0.71073	0.71073	0.71073
Crystal size (mm)	$0.24 \times 0.12 \times 0.08$	$0.18 \times 0.10 \times 0.05$	$0.44 \times 0.10 \times 0.10$
Color	red	orange	brown
μ(Mo Kα) (mm^{-1})	3.711	10.667	0.844
Collection range (°)	$1.39 \leqslant \theta \leqslant 23.28$	$2.02 \leqslant \theta \leqslant 23.36$	$1.64 \leqslant \theta \leqslant 23.29.$
Correction factors (SADABS) min/max	0.749272	0.344129	0.805463
Reflections collected	6260	3387	8928
Independent reflections [R(int)]	2056 [0.0382]	2144 [0.0213]	2779 [0.0257]
Reflections observed, $I > 2\sigma(I)$	1512	1929	2394
Goodness-of-fit on F^2	0.992	1.001	1.045
Number of parameters	194	191	234
Residuals R, wR_2 (all)	0.0337, 0.0831	0.0298, 0.0779	0.0268, 0.0650

Table 1b
Crystal data and refinement details for **3a**, **3c** and **4a**

	3a	**3c**	**4a**
Empirical formula	$C_{13}H_{12}BrMnN_2O_5$	$C_{16}H_{19}ClMoN_2O_4$	$C_{16}H_{10}BrMnN_2O_5$
Formula weight	411.10	533.67	445.11
Crystal system	triclinic	monoclinic	triclinic
Space group	$P\bar{1}$	$P2(1)$	$P\bar{1}$
a (Å)	7.0213(15)	9.1017(19)	8.213(3)
b (Å)	9.770(2)	9.408(2)	12.115(5)
c (Å)	13.955(3)	10.612(2)	21.579(8)
α (°)	92.118(4)	90	82.058(7)
β (°)	100.150(4)	93.593(4)	86.561(8)
γ (°)	102.082(3)	90	84.997(8)
V (Å^3)	918.7(3)	906.9(3)	969.8(8)
Z	2	2	4
T (K)	298(2)	298(2)	296(2)
D_{calc} (g cm^{-3})	1.486	1.592	1.397
$F(000)$	408	440	880
λ (Mo Kα) (Å)	0.71073	0.71073	0.71073
Crystal size (mm)	$0.25 \times 0.22 \times 0.05$	$0.18 \times 0.14 \times 0.04$	$0.27 \times 0.13 \times 0.03$
Color	orange	dark red	red
μ(Mo Kα), mm^{-1}	2.912	0.892	2.535
Collection range (°)	$1.49 \leqslant \theta \leqslant 28.30$	$1.92 \leqslant \theta \leqslant 23.30$	$0.95 \leqslant \theta \leqslant 23.33$
Correction factors (SADABS) min/max	0.598363	0.727477	0.550227
Reflections collected	8877	5922	9587
Independent reflections [R(int)]	4446 [0.0415]	2597 [0.0344]	6043 [0.0640]
Reflections observed, $I > 2\sigma$ (I)	2665	2304	2672
Goodness-of-fit on F^2	1.042	1.008	1.052
Number of parameters	203	221	454
Residuals R, wR_2 (all)	0.0560, 0.1918	0.0314, 0.0628	0.0817, 0.2588

MeOH (3 ml) for 3 h. The solvent was evaporated *in vacuo*, and the resulting solid residue was dissolved in THF and filtered through kieselguhr. Addition of hexane and slow evaporation at reduced pressure gave compound **2c** as dark blue microcrystals. Yield: 0.118 g, 82%. Anal. Calc. for $C_{15}H_{17}ClMoN_2O_4$: C, 42.82; H; 4.07; N; 6.66. Found: C,

Table 2
Selected distances (Å) and angles (°) for compounds

	2a X = Br M = Mn	**2b** X = Br M = Re	**2c** X = Cl M = Mo	**3a** X = Br M = Mn	**3c** X = Cl M = Mo	**4a** X = Br M = Mn
M–X	2.5271(11)	2.621(2)	2.5028(9)	2.5352(11)	2.5027(17)	2.524(3)
M–N(1)	2.041(4)	2.169(6)	2.237(2)	2.048(5)	2.237(4)	2.053(11)
M–N(2)	2.047(4)	2.157(6)	2.256(2)	2.041(4)	2.260(4)	2.056(12)
M–C(1)O	1.829(6)	1.919(9)	1.809(9)	1.791(7)	1.957(7)	1.80(2)
M–C(2)O	1.816(6)	1.923(9)	1.955(4)	1.803(7)	1.946(7)	1.815(18)
M–C(3)O	1.803(6)	1.894(9)		1.791(7)		1.83(2)
N(1)–M–N(2)	78.49(15)	75.0(2)	73.56(9)	78.35(18)	72.96(15)	77.5(5)

Table 3
^{1}H NMR data for the pyridylimino and acid protons

	2a	**2b**	**2c**	**3a**	**3b**	**3c**	**4a**	**4b**	**4c**
δH_1	8.90	9.25	8.80	8.82	9.22	8.74	8.97	9.40	8.94
δH_3	8.21	8.32	8.07	8.19	8.32	8.07	8.36	8.49	8.28
δH_4	8.21	8.32	8.15	8.19	8.34	8.16	8.14	8.40	8.25
δH_5	7.76	7.82	7.68	7.75	7.81	7.68	7.77	7.91	7.77
δH_6	9.25	9.11	8.79	9.25	9.10	8.79	9.34	9.19	8.89
δH_{acid}	10.65	10.70	10.87	10.80	10.78	10.59	11.43	11.66	11.62

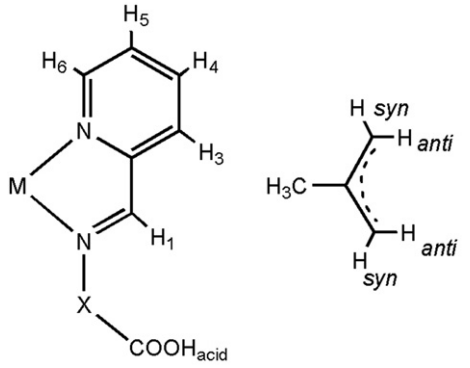

Fig. 6. Atom labeling scheme used at the NMR studies for the piridylimino and allyl ligands.

42.44; H, 3.98; N, 6.35%. IR (THF), *v*(CO): 1952 (vs), 1874 (s), 1734 (m) (acid) cm^{-1}. ^{1}H NMR (acetone-d_6): δ 10.87 (br, 1H, COO*H*), 8.80 (s, 1H, –C*H*=N–), 8.79 [d(7), 1H, H^6 py], 8.15 [t(7), 1H, H^4 py], 8.07 [d(7), 1H, H^3 py], 7.68 [t(6), 1H, H^5 py], 4.17 (m, 2H, H^2 NCH_2), 3.02 (m, 2H, CH_2COOH), 2.94 [d(3), 1H, H_{syn} allyl], 2.80 [d(3), 1H, H_{syn} allyl], 1.32 (s, 3H, CH_3), 1.21 (s, 1H, H_{anti} allyl), 1.16 (s, 1H, H_{anti} allyl).

*3.5. Synthesis of [MnBr(CO)$_3${py-2-CH=N–(CH$_2$)$_3$–COOH}] (**3a**)*

Compound **1a** [16] (0.120 g, 0.370 mmol) and GABA (γ-aminobutyric acid) (0.038 g, 0.370 mmol) were refluxed in EtOH (25 ml) for 1 h. The solvent was evaporated *in vacuo*, and the resulting solid residue was dissolved in THF and filtered through kieselguhr. Addition of hexane and slow evaporation at reduced pressure gave compound **3a** as orange microcrystals. Yield: 0.128 g, 84%. Anal. Calc. for $C_{13}H_{12}BrMnN_2O_5$: C, 37.98; H, 2.94; N, 6.81. Found: C, 38.26; H, 2.77; N, 6.59%. IR (THF), *v*(CO): 2024 (vs), 1938 (s), 1916 (s), 1735 (m) (acid) cm^{-1}. ^{1}H NMR (acetone-d_6): δ 10.80 (br, 1H, COO*H*), 9.25 [d(5), 1H, H^6 py], 8.82 (br, 1H, –C*H*=N–), 8.19 (m, 2H, $H^{3,4}$ py), 7.75 [t(6), 1H, H^5py], 4.30 (br, 2H, NCH_2), 2.48 (br, 2H, CH$_2$CH_2CH$_2$), 2.36 (br, 2H, CH_2COOH).

*3.6. Synthesis of [ReBr(CO)$_3${py-2-CH=N–(CH$_2$)$_3$–COOH}] (**3b**)*

Compound **1b** [16] (0.120 g, 0.262 mmol) and GABA (γ-aminobutyric acid) (0.027 g, 0.262 mmol) were refluxed in EtOH (25 ml) for 1 h. The solvent was evaporated *in vacuo*, and the resulting solid residue was dissolved in THF and filtered through kieselguhr. Addition of hexane and slow evaporation at reduced pressure gave compound **3b** as orange microcrystals. Yield 0.114 g, 80%. Anal. Calc. for $C_{13}H_{12}BrN_2O_5Re$: C, 28.79; H, 2.23; N, 5.17. Found: C, 28.96; H, 2.49; N, 4.99%. IR (THF), *v*(CO): 2021 (vs), 1923 (s), 1898 (s), 1736 (m) (acid) cm^{-1}. ^{1}H NMR (acetone-d_6): δ 10.78 (br, 1H, COO*H*), 9.22 (s, 1H, –C*H*=N), 9.10 [d(5), 1H, H^6 py], 8.34 (m, 1H, H^4 py), 8.32 (m, 1H, H^3 py),7.81 (m, 1H, H^5 py), 4.26 [t(7), 2H, NCH_2], 2.50 (m, 2H, CH$_2$CH_2CH$_2$), 2.33 (m, 2H, CH_2COOH).

*3.7. Synthesis of [MoCl(η^3-C$_3$H$_4$Me-2)(CO)$_2${py-2-CH=N-(CH$_2$)$_3$–COOH}] (**3c**)*

Compound **1c** [16] (0.120 g, 0.343 mmol) and GABA (γ-aminobutyric acid) (0.035 g, 0.343 mmol) were refluxed in THF (25 ml) and MeOH (3 ml) for 3 h. The solvent was evaporated *in vacuo*, and the residue resulting solid

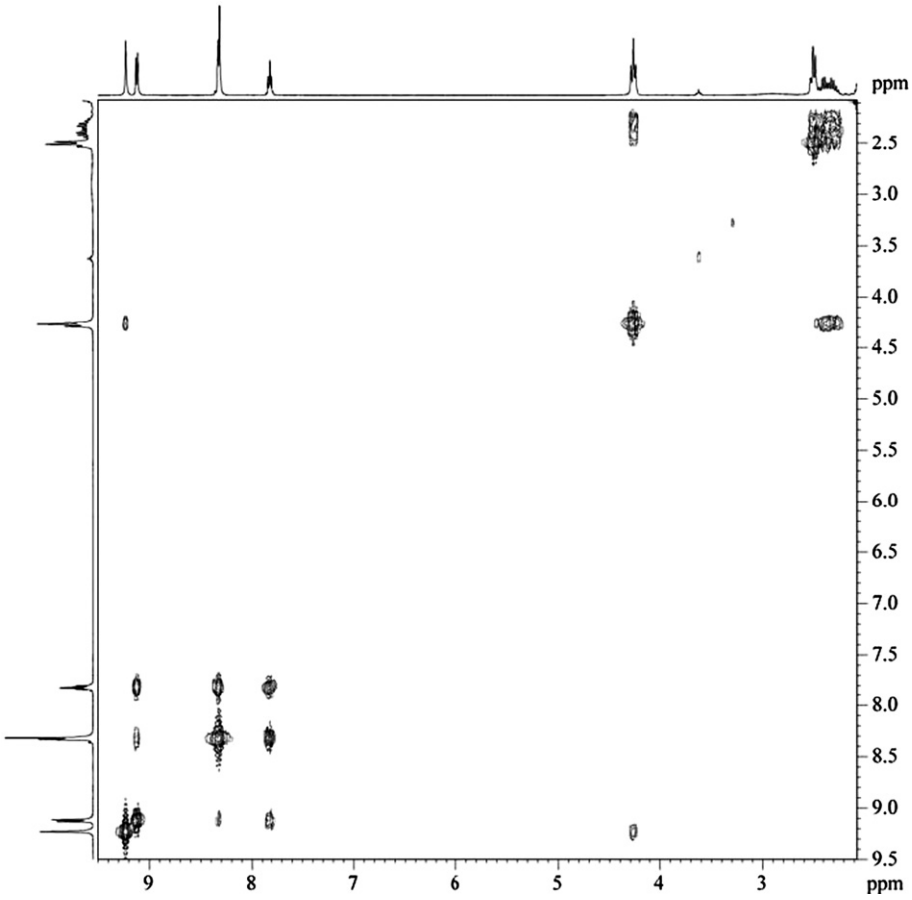

Fig. 7. ^{1}H–^{1}H COSY NMR experiment for complex **3b** in acetone-d_6 at 20 °C.

residue was dissolved in THF and filtered through kieselguhr. Addition of hexane and slow evaporation at reduced pressure gave compound **3c** as dark blue microcrystals Yield: 0.122 g, 82%. Anal. Calc. for $C_{16}H_{19}ClMoN_2O_4$: C, 44.20; H, 4.40; N, 6.44. Found: C, 44.54; H, 4.58; N, 6.33%. IR (THF), *v*(CO): 1952 (vs), 1874 (s), 1735 (m) (acid) cm^{-1}. ^{1}H NMR (acetone-d_6): δ 10.59 (br, 1H, COO*H*), 8.79 [d(5), 1H, H^6 py], 8.74 (s, 1H, –C*H*=N–), 8.16 [td(8,2), 1H, H^4 py], 8.07 [d(7), 1H, H^3 py], 7.68 (m, 1H, H^5 py), 4.13 (m, 1H, NCH_2), 3.83 (m, 1H, NCH_2), 2.96 [d(3), 1H, H_{syn} allyl], 2.78 [d(3), 1H, H_{syn} allyl], 2.43 (m, 2H, $CH_2CH_2CH_2$), 2.19 (m, 2H, CH_2COOH) 1.34 (s, 3H, CH_3), 1.21 (s, 1H, H_{anti} allyl), 1.13 (s, 1H, H_{anti} allyl).

3.8. Synthesis of [MnBr(CO)$_3$(py-2-CH=N–C$_6$H$_4$-m-COOH)] (*4a*)

Compound **1a** [16] (0.120 g, 0.370 mmol) and 3-aminobenzoic acid (0.051 g, 0.370 mmol) were refluxed in EtOH (25 ml) for 1 h. The solvent was evaporated *in vacuo*, and the resulting solid residue was dissolved in THF and filtered through kieselguhr. Addition of hexane and slow evaporation at reduced pressure gave compound **4a** as red-orange microcrystals. Yield: 0.139 g, 85%. Anal. Calc. for: $C_{16}H_{10}BrMnN_2O_5$: C, 43.18; H, 2.26; N, 6.29. Found: C, 43.32; H, 2.47; N, 5.95%. IR (THF), *v*(CO): 2026 (vs), 1944 (s), 1919 (s), 1724 (m) (acid) cm^{-1}. ^{1}H NMR (acetone-d_6): δ 11.43 (br, 1H, COO*H*), 9.34 [d(3), 1H, H^6 py], 8.97 (br, 1H, –C*H*=N–), 8.36 (m, 1H, H^3 py), 8.31 (m, 2H, $H^{2,6}$ Ph), 8.14 (m, 1H, H^4 py), 7.87 (m, 2H, $H^{4,5}$ Ph), 7.77 (m, 1H, H^5 py).

3.9. Synthesis of [ReBr(CO)$_3$(py-2-CH=N–C$_6$H$_4$-m-COOH)] (*4b*)

Compound **1b** [16] (0.120 g, 0.262 mmol) and 3-aminobenzoic acid (0.036 g, 0.262 mmol) were refluxed in EtOH (25 ml) for 1 h. The solvent was evaporated *in vacuo*, and the resulting solid residue was dissolved in THF and filtered through kieselguhr. Addition of hexane and slow evaporation at reduced pressure gave compound **3b** as orange microcrystals. Yield 0.127 g, 84%. Anal. Calc. for: $C_{16}H_{10}BrN_2O_5Re$: C, 33.34; H, 1.75; N, 4.86. Found: C, 33.64; H, 1.96; N, 4.77%. IR (CH_2Cl_2), *v*(CO): 2024 (vs), 1927 (s), 1901 (s), 1724 m (acid) cm^{-1}. ^{1}H NMR (acetone-d_6): δ 11.66 (br, 1H, COO*H*), 9.40 (s, 1H, –C*H*=N–), 9.19 [d(5), 1H, H^6 py], 8.49 [d(7), 1H, H^3 py], 8.40 [td (7, 1), 1H, H^4 py], 8.26 (s, 1H, H^2 Ph), 8.14 [d(8), 1H, H^6 Ph], 7.95 (m, 1H, H^5 py), 7.91 (m, 1H, H^4 Ph), 7.74 [t(8), 1H, H^5 Ph].

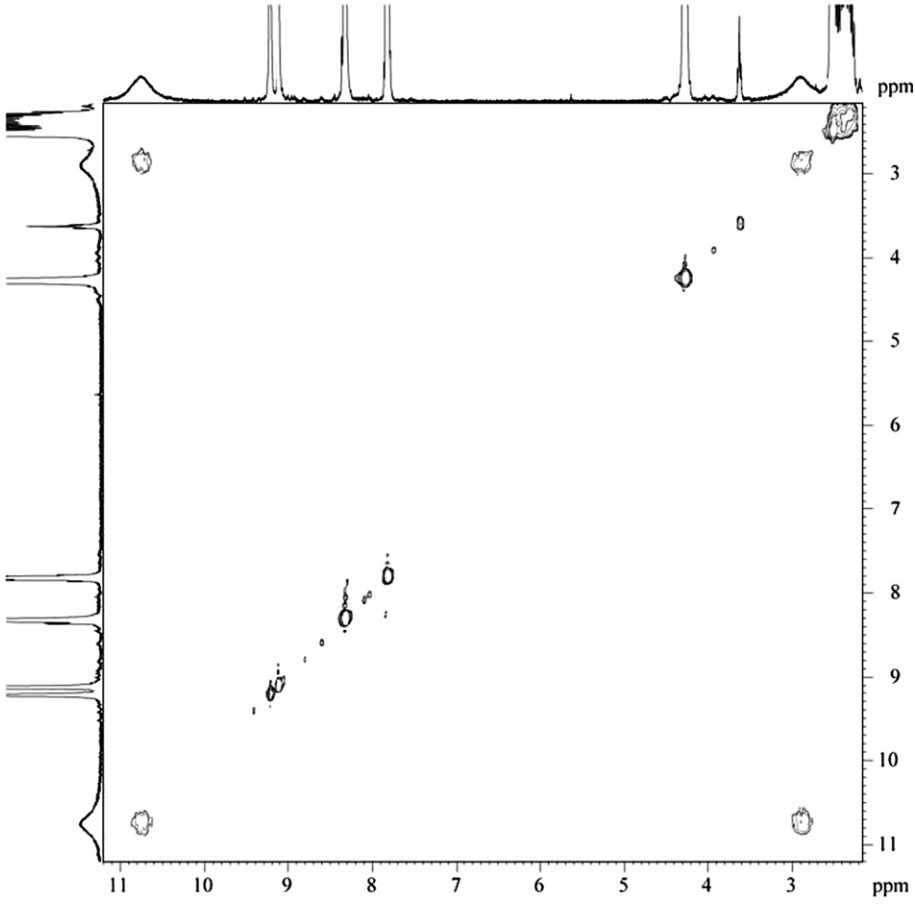

Fig. 8. ^{1}H–^{1}H EXSY NMR experiment of complex **3b** in acetone-d_6 at 20 °C.

3.10. Synthesis of [MoCl(η^3-C_3H_4Me-2)(CO)$_2$-(py-2-CH=N–C_6H_4-m-COOH)] (**4c**)

Compound **1c** [16] (0.120 g, 0.343 mmol) and 3-aminobenzoic acid (0.047 g, 0.343 mmol) were refluxed in THF (25 ml) and MeOH (3 ml) for 30 min. The solvent was evaporated *in vacuo*, and the resulting solid residue was dissolved in THF and filtered through kieselguhr. Addition of hexane and slow evaporation at reduced pressure gave compound **2c** as dark blue microcrystals. Yield: 0.132 g, 82%. Anal. Calc. for $C_{19}H_{17}ClMoN_2O_4$: C, 48.68; H, 3.66; N, 5.98. Found: C, 48.93; H, 3.89; N, 5.91%. IR (THF), ν(CO): 1953 (vs), 1877 (s), 1722 (m) (acid) cm^{-1}. ^{1}H NMR (acetone-d_6): δ 11.62 (br, 1H, COO*H*), 8.94 (s, 1H, –C*H*=N–), 8.89 [d(5), 1H, H^6 py], 8.28 [d(2), 1H, H^3 py], 8.25 [d(2), 1H, H^4 py], 8.21 (s, 1H, H^2 Ph), 8.10 [d(8), 1H, H^6 Ph], 7.97 [d(8), 1H, H^4 Ph], 7.77 (m, 1H, H^5 py), 7.68 [t(8), 1H, H^5 Ph], 2.90 [d(3), 1H,H_{syn} allyl], 2.22 [d(3), 1H,H_{syn} allyl], 1.42 (s, 3H, CH_3), 1.27 (s, 1H, H_{anti} allyl), 1.04 (s, 1H, H_{anti} allyl).

3.11. X-ray crystallography

Crystals suitable for diffraction studies were grown by slow diffusion of hexane into THF solutions (for **2a**, **2b**, **3a** and **4a**) or 5: 1 mixture of THF: Methanol (for **2c** and **3c**) at −20 °C. Data for were collected on a Bruker Smart 1000 CCD diffractometer (graphite-monochromatized Mo Kα radiation, $\lambda = 0.71073$Å). Crystallographic data and experimental details for the structures are summarized in Table 1. Raw frame data were integrated with SAINT [26]. A semi-empirical absorption correction was applied with SADABS [27]. The structures were solved by direct methods with SIR2002 [28] under WINGX [29] and refined against F^2 with SHELXTL [30]. All non-hydrogen atoms were refined anisotropically. Hydrogen atoms were set in calculated positions and refined as riding atoms, with a common thermal parameter. Graphics were made with SHELXTL. Additional calculations were made with PARST [31].

Acknowledgements

We thank the Spanish MEC (CTQ-2006-08924) and JCyL (VA012C05) for financial support. In addition, R.G.-R and C. M. A. wish to thank Ministerio de Educación y Ciencia for a MEC-FPU grant and a Ramón y Cajal contract respectively.

Appendix A. Supplementary data

CCDC 664387, 664388, 664389, 664390, 664391 and 664392 contain the supplementary crystallographic data

for **2a**, **2b**, **2c**, **3a**, **3c** and **4a**. These data can be obtained free of charge from The Cambridge Crystallographic Data Centre via www.ccdc.cam.ac.uk/data_request/cif. Supplementary data associated with this article can be found, in the online version, at doi:10.1016/j.jorganchem.2007.09.025.

References

[1] (a) D.R. van Staveren, N. Metzler-Nolte, Chem. Rev. 104 (2004) 5931;
(b) G. Jaouen, A. Vessieres, I.S. Butler 26 (1993) 361.
[2] (a) M. Albrecht, G. VanKoten, Angew. Chem. Int. Ed. 40 (2001) 3750;
(b) G. Guillena, G. Rodríguez, M. Albrecht, G. VanKoten, Chem. Eur. J. 8 (2002) 5638.
[3] M. Salmain, A. Vessieres, P. Brossier, I.S. Butler, G. Jaouen, J. Pharm. Biomed. Anal. 21 (1999) 625.
[4] J. Wang, Electroanalysis 13 (2001) 983.
[5] (a) J.K. Pak, P. Benny, B. Spingler, K. Ortner, R. Alberto, Chem. Eur. J. 9 (2003) 2053;
(b) R. Alberto, K. Ortner, N. Wheatley, R. Schibli, A.P. Schubiger, J. Am. Chem. Soc. 123 (2001) 3135;
(c) J. Petrig, R. Schibli, C. Dumas, R. Alberto, A.P. Schubiger, Chem. Eur. J. 7 (2001) 1868;
(d) J.D.G. Correia, A. Domingos, I. Santos, R. Alberto, K. Ortner, Inorg. Chem. 40 (2001) 5147;
(e) R. Alberto, R. Schibli, R. Waibel, U. Abram, A.P. Schubiger, Coord. Chem. Rev. 190–192 (1999) 901.
[6] (a) L. Pu, Chem. Rev. 104 (2004) 1687;
(b) K.K.W. Lo, W.K. Hui, D.C.M. Ng, J. Am. Chem. Soc. 124 (2002) 9344;
(c) M.K. Brennaman, J.H. Alstrum-Acevedo, C.N. Fleming, P. Jang, T.J. Meyer, J.M. Papanikolas, J. Am. Chem. Soc. 124 (2002) 15094.
[7] R. García-Rodríguez, D. Miguel, Dalton Trans. (2006) 1218.
[8] (a) L. Barisic, M. Cakic, K.A. Mahmoud, Y. Liu, H.B. Kraatz, H. Pritzkow, S.I. Kirin, N. Metzler-Nolte, V. Rapic, Chem. Eur. J. 12 (2006) 4965;
(b) U. Hoffmanns, N. Metzler-Nolte, Bioconjugate Chem. 17 (2006) 204;
(c) D.R. van Staveren, N. Metzler-Nolte, Chem. Commun. (2002) 1406.
[9] A. Vessieres, M. Salmain, P. Brossier, Biomed. Anal. 21 (1999) 651.
[10] J.M. Lehn, Supramolecular Chemistry: Concepts and Perspectives, VCH, Weinheim, 1995.
[11] (a) M.A. Cinellu, S. Stoccoro, G. Minghetti, A.L. Bandini, G. Banditelli, B. Bovio, J. Organomet. Chem. 372 (1989) 311;
(b) M. Munakata, L.P. Wu, M. Yamamoto, T. Kuroda-Sowa, M. Maekawa, S. Kawata, S. Kitagawa, J. Chem. Soc., Dalton Trans. (1995) 4099;
(c) G.A. Ardizzoia, G. La Monica, S. Cenini, M. Moret, N. Maschioni, J. Chem. Soc., Dalton Trans. (1996) 1351;
(d) I.A. Guzei, C.H. Winter, Inorg. Chem. 36 (1997) 4415;
(e) S.M. Couchman, J.C. Jeffery, M.D. Ward, Polyhedron 18 (1999) 2633.
[12] (a) G.R. Desiraju, Angew. Chem. Int. Ed. 34 (1995) 2311;
(b) D. Das, G.R. Desiraju, Chem. Asian J. 1–2 (2006) 231;
(c) G.R. Desiraju, J. Mol. Struct. 656 (2003) 5.
[13] (a) D. Braga, F. Grepioni, Acc. Chem. Res. 33 (2000) 601;
(b) D. Braga, F. Grepioni, G.R. Desiraju, J. Organomet. Chem. 548 (1997) 33.
[14] K. Heinze, V. Jacob, J. Chem. Soc., Dalton Trans. (2000) 2379.
[15] W. Wang, B. Spingler, R. Alberto, Inorg. Chim. Acta 355 (2003) 386.
[16] C.M. Alvarez, R. García-Rodríguez, D. Miguel, Dalton Trans. (2007) 3546.
[17] M. Sanderg, I.J. Jacobson, Neurochemistry 37 (1981) 1353.
[18] (a) T. Horikoshi, A. Asanuma, K. Yanagisawa, K. Anzai, S. Goto, Mol. Brain Res. 4 (1988) 97;
(b) D. Choquet, H. Korn, Neuroscience Lett. 84 (1988) 329;
(c) F.S. Wu, T.T. Gibbs, D.H. Farb, Eur. J. Pharmacol. 246 (1993) 239.
[19] B.P. Buffin, P.J. Sqattrito, A.O. Ojewole, Inorg. Chem. Commun. 2 (2004) 14.
[20] R.S. Herrick, J. Dupont, I. Wrona, J. Pilloni, M. Beaver, M. Benotti, F. Powers, C.J. Ziegler, J. Organomet. Chem. 692 (2007) 1226.
[21] C.M. Jung, W. Kraus, P. Leibnitz, H.J. Pietzsch, J. Kropp, H. Spies, Eur. J. Inorg. Chem. (2002) 1219.
[22] (a) R.S. Herrick, K. L Houde, J.S. McDowell, L.P. Kizeck, G. Bonavia, J. Organomet. Chem. 589 (1999) 29;
(b) R.S. Herrick, I. Wrona, N. McMicken, G. Jones, C.J. Ziegler, J. Shaw, J. Organomet. Chem. 689 (2004) 4848.
[23] L.A. García-Escudero, D. Miguel, J.A. Turiel, J. Organomet. Chem. 691 (2006) 3434.
[24] The crystal of the hydrate, and hence the structural determination, were of poor quality and therefore the structure is not presented here. More details can be obtained fron the authors on request.
[25] G. Barrado, M.M. Hricko, D. Miguel, V. Riera, H. Wally, S. García-Granda, Organometallics 17 (1998) 820.
[26] SAINT+. SAX area detector integration program. Version 6.02. Bruker AXS, Madison, WI, 1999.
[27] G.M. Sheldrick, SADABS, Empirical Absorption Correction Program, University of Göttingen, Göttingen, Germany, 1977.
[28] M.C. Burla, M. Camalli, B. Carrozzini, G.L. Cascarano, C. Giacovazzo, G. Polidory, R. Spagna, SIR2002, A program for automatic solution and refinement of crystal structures. A. Altomare, M.C. Burla, M. Camalli, G.L. Cascarano, C. Giacovazzo, A. Guagliardi, A.G.G. Moliterni, G. Polidori and R. Spagna, J. Appl. Crystallogr. 32 (1999) 115.
[29] L.J. Farrugia, J. Appl. Crystallogr. 32 (1999) 837.
[30] G.M. Sheldrick, SHELXTL, An integrated system for solving, refining, and displaying crystal structures from diffraction data. Version 5.1. Bruker AXS, Inc. Madison, WI, 1998.
[31] (a) M. Nardelli, Comput. Chem. 7 (1983) 95;
(b) M. Nardelli, J. Appl. Crystallogr. 28 (1995) 659.